The 2009 IEEE/RSJ International Conference on
Intelligent Robots and Systems
October 11-15, 2009 St. Louis, USA

A Controller for Dynamic Walking in Bipedal Robots

David J. Braun and Michael Goldfarb, *Member, IEEE*

Abstract— **This paper presents an approach for the closed-loop control of actuated biped that allows natural looking and energy efficient walking. Rather than prescribe kinematic trajectories or kinematic constraints, the approach is based on the prescription of state dependent torques that "encourage" patterned movement. Some of the prescribed torques are referenced to the inertial reference frame, which largely decouples the angular dynamics of the robot, and as such greatly simplifies the selection of control parameters. Implementation of torques from the inertial coordinate frames is enabled by a joint torque computation which is motivated by Gauss's principle of least constraint. The proposed approach is implemented in simulation on an anthropomorphic biped, and is shown to quickly converge to a natural looking gait limit cycle. Simulations are conducted with various control parameters and different initial conditions. The authors also show that walking speed can be altered in a simple manner by varying two intuitive controller parameters. The mechanical cost of transport computed on a representative dynamic walk is used to validate energy efficiency of the proposed control approach.**

Index Terms— **Legged Robots; Dynamics.**

I. Introduction

Recent literature on the topic of walking robots describes two fundamentally different approaches for achieving bipedal locomotion. Perhaps, the most comprehensively developed is the ZMP approach, which utilizes trajectory tracking to control the motion of the robot, [1], [2], [3], [4], [5], [6]. This type of approach provides versatility and robustness in gait, but since it prescribes and tracks trajectories, it overrides the natural dynamics of the walking robot, which results in a stiff and unnatural looking gait with a concomitant low efficiency [7].

On the other hand, one can leverage the natural dynamics of the robot, and attempts to use these dynamics as the basis for a stable limit cycle that will result in locomotion. This approach to locomotion includes fully passive walkers, [8], [9], [10], actuator-assisted walkers based largely on passive versions, [11] and [12], and actuated walkers that utilize control approaches in order to leverage some open-loop dynamic behavior, [13], [14], [15], [16]. One form of the latter is the work by Pratt et al. [17], which imposes virtual forces rather than kinematic constraints on the robot, and thus need not override the open-loop dynamics of the biped. Such an approach additionally enables a reasonably intuitive manner in which to control the biped. However, the virtual Cartesian forces imposed on the body center of mass interfere with the "natural" motion of the robot. That is, the motion of the robot should result from the dynamic interaction between the body, legs, and ground, (i.e., the body should "ride" atop the legs, and should not otherwise be pushed or pulled in a Cartesian sense).

This paper presents a control approach that enables dynamic biped walking on an actuated robot, which can provide a more efficient gait than trajectory tracking approaches. Rather than prescribing a kinematics (i.e., joint angle trajectories), the approach subjects the robot to a set of state-dependent torques. These torques are constructed from angular springs and dampers with fixed equilibrium points, which influence the natural dynamics to generate a stable gait. The present approach references some of these torques to an inertial reference frame and others to the internal robot frame; and develops a model-based solution for joint torques utilizing the Gauss principle of least constraint [23], [24].

The proposed modeling and control framework does not neglect the foot of the robot and in this context provides a nontrivial extension to the works [13], [14], [15]. Moreover, we relax a usual flat-foot assumptions made by other control approaches such as ZMP, which can be consider as another nontrivial extension on large body of control methods previously presented in literature. It is also important to point out that unlike other approaches applied on actuated biped robots, the presented one neither enforces predefined trajectory nor dictates any other time, position, or velocity based attribute of the walking-cycle (i.e., desired walking speed, stepping frequency or step length). Rather, all such gait characteristics are obtained indirectly by the interaction between the robot and environment under the influence of the control forces.

The proposed control approach, the application of which leads to an energy efficient and natural looking dynamic walk, is described herein and subsequently demonstrated via simulation.

II. Biped Model

The control methodology is based upon a dynamic model of the robot introduced in this section. This model is derived by means of the Gauss principle of least constraint utilizing the Udwadia-Kalaba approach [18]. Unlike traditionally used biped models derived separately for single support, double support and "flight" phase, the present model offers a unified representation which is valid for all phases of gait. The proposed analytical description of the biped dynamics which is

The autors are with the Department of Mechanical Engineering, Vanderbilt University, Nashville, TN 37235 USA (david.braun@vanderbilt.edu; michael.goldfarb@vanderbilt.edu).

This paper has supplementary downloadable multimedia material provided by the authors. This material includes a video (walking video.mpeg) demonstrating dynamic bipedal walk coordinated by the proposed controller. The video can be played with Windows Media Player. The total size is 4 MB.

valid under redundant constraints and kinematic singularities, allows the formulation of a control methodology with no restriction on biped configuration.

In order to facilitate model and controller development, both are developed in the context of a seven-link (nine degree-of-freedom) planar biped, as illustrated in Fig. 1. The configuration of the biped is defined with the generalized coordinates, $\mathbf{q} = [x, y, \theta, \theta_1, \theta_2, \theta_3, \theta_4, \theta_5, \theta_6]^T$, defined relative to the inertial reference frame. The biped is assumed to be actuated at each joint (i.e., right and left hip, knee, and ankle joints), such that, the dynamics of the robot are affected by the joint torques, $\mathbf{u} = [u_1, u_2, u_3, u_4, u_5, u_6]^T$, which are assumed positive in the same direction as the joint angles.

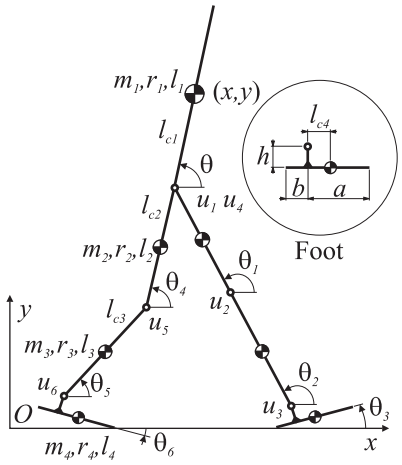

Fig. 1. Seven-link biped with generalized coordinates and associated geometric and inertial properties. The corresponding links on both legs are geometrically and inertially identical. For each segment, the moment of inertia with respect to the center of mass of the associated link is calculated as $I_* = m_* r_*^2$.

A. Unconstrained Dynamics

Consider an n-dof autonomous multibody system, the configuration of which is uniquely specified by $\mathbf{q} \in \Re^n$ generalized coordinates. The equations of motion, for the unconstrained "flying" biped, can be written as:

$$\mathbf{M}(\mathbf{q})\ddot{\mathbf{q}} + \mathbf{h}(\mathbf{q}, \dot{\mathbf{q}}) + \mathbf{G}(\mathbf{q}) = \mathbf{Q}_u, \tag{1}$$

where $\mathbf{M} \in \Re^{n \times n}$ is a symmetric and positive definite mass matrix, $\mathbf{h} \in \Re^n$ represents the normal and Coriolis inertial forces, $\mathbf{G} \in \Re^n$ represents the gravitional forces, while $\mathbf{E} \in \Re^{n \times m}$ is a matrix mapping control inputs $\mathbf{u} \in \Re^m$ to generalized actuator force space $\mathbf{Q}_u = \mathbf{E}\mathbf{u}$.

B. Kinematic Constraints

For the biped in Fig.1, neither foot can penetrate the ground, the knee joints cannot extend beyond the fully straight position, and both feet are assumed not to slide when in contact with the ground. Since each toe and heel are independently characterized by non-penetration and no-slip with the ground, the biped dynamics can be subject to ten (dependent) kinematic constraints. Following a general notation, the set of kinematic constraints imposed on the biped is given by:

$$\mathbf{\Phi} = [\mathbf{\Phi}_h(\mathbf{q})^T, \mathbf{\Phi}_n(\mathbf{q}, \dot{\mathbf{q}})^T]^T = \mathbf{0}, \tag{2}$$

where $\mathbf{\Phi}_h$ represents the holonomic constraints (e.g., the non-penetration between the toe and heel and the ground, or the full extension of the knee joint), and $\mathbf{\Phi}_n$ represents the nonholonomic constraints (i.e., the non-slip condition between each foot and the ground).

We assume that $\mathbf{\Phi}_h$ is twice and $\mathbf{\Phi}_n$ is at least once differentiable while the initial conditions are constraint consistent. In this case, (2) can be equivalently represented as:

$$\mathbf{A}(\mathbf{q})\ddot{\mathbf{q}} = \mathbf{b}(\mathbf{q}, \dot{\mathbf{q}}), \tag{3}$$

where, $\mathbf{A} = [\mathbf{A}_h^T, \mathbf{A}_n^T]^T$ is the constraint matrix defined in terms of $\mathbf{A}_h = \partial\mathbf{\Phi}_h/\partial\mathbf{q}$ and $\mathbf{A}_n = \partial\mathbf{\Phi}_n/\partial\dot{\mathbf{q}}$, while $\mathbf{b} = \mathbf{A}\ddot{\mathbf{q}} - [\ddot{\mathbf{\Phi}}_h^T, \dot{\mathbf{\Phi}}_n^T]^T$, [19]. Note that when a constraint becomes inactive (as a function of system configuration), it is eliminated by zeroing the corresponding row in (3). On the other hand, when a constraint switches from passive to active (e.g., during ground contact or when the knee hits a full extension stop), engagement of the constraint will impart an impact to the system dynamics.

C. Constrained Dynamics

Based on the Gauss principle of least constraint [20], [19], the constrained acceleration $\ddot{\mathbf{q}}$, which satisfies (3), can be obtained from:

$$\ddot{\mathbf{q}} = \mathbf{a} + \mathbf{R}^{-1}\mathbf{C}^{+}(\mathbf{b} - \mathbf{A}\mathbf{a}), \tag{4}$$

where $\mathbf{a} = \mathbf{M}^{-1}(\mathbf{Q}_u - \mathbf{h} - \mathbf{G})$ is the acceleration the system would have without the imposed constraints (2)), $\mathbf{R}$ is defined as the upper triangular Cholesky factorization of the mass matrix $\mathbf{M} = \mathbf{R}^T\mathbf{R}$, [21], $\mathbf{C} = \mathbf{A}\mathbf{R}^{-1}$, is the weighted constraint matrix, while $\mathbf{C}^+$ is the pseudoinverse (i.e., the Moore-Penrose inverse) of $\mathbf{C}$ [22]. This formulation explicitly defines the acceleration of the constrained motion, which is well defined under dependent constraints, see [18].

III. Selecting Torques for Dynamic Walking

Our objective in walking is to maintain an upright body position, and also to sustain a stable oscillation in leg motion characterized by a ballistic component in swing. The first objective, to maintain an (essentially) upright body position, can be achieved by prescribing a torque that attracts the torso to a nominally vertical position. In order to drive leg oscillation, the thigh segments are subjected to alternating torques, where the alternation is driven by changes in biped configuration (e.g., heel strike and heel off). Specifically, during swing phase, the prescribed torque drives hip flexion by attracting the thigh segment toward a given (flexion) angular orientation. Upon heel strike, another torque drives hip extension by attracting the thigh segment toward a given (extension) angular orientation.

During swing, the knee is not subject to a driving torque, but rather is subject only to damping (and as such, the swing leg dynamics are in essence ballistic). During early stance

phase (i.e., heel strike to heel off) a somewhat stiff spring maintains the knee in a fully extended position. The ankle is subject to a torque during swing that encourages slight flexion (to prevent stumbling), and to one during stance that generates a slight push-off before the stance leg enters swing.

The torso and the thigh segment torques are defined relative to the inertial reference frame, while the knee and ankle torques are defined relative to the respective adjacent links. The respective torques attract the three segments (i.e., the torso, right thigh, and left thigh) each to a respective angular configuration, and as such, the angular dynamics of the biped is mainly reduced to three decoupled and relatively low-order dynamic subsystems (i.e., two inverted pendulums and one non-inverted double pendulum). Achieving a desired (angular) dynamics in each of these subsystems is considerably simpler than considering the fully coupled system.

A. Transforming the Desired Control Torques to the Actuator Space

In order to implement the presented approach, we propose a transformation between the desired generalized control torques and the joint torques as follows. The objective of the transformation is to achieve the same constrained motion forcing the dynamics (1), (2) with $\mathbf{Q}_u = \mathbf{E}\mathbf{u}$ as would be achieved with the application of a set of desired generalized actuator forces $\mathbf{Q}_d$. Denoting the desired constrained acceleration as $\ddot{\mathbf{q}}_d$ and the constrained acceleration generated by the actuator torques as $\ddot{\mathbf{q}}$, the objective of the transformation can be stated as $\ddot{\mathbf{q}} = \ddot{\mathbf{q}}_d$. This equivalence relation, however, cannot be realized exactly on underactuated motion phases (i.e., if only a toe or a heel touches the ground in single support phase). To handle this issue, we propose a general formulation to define the joint torques:

$$\mathbf{u} = min\{\mathbf{u} \in \Re^m : (\ddot{\mathbf{q}} - \ddot{\mathbf{q}}_d)^T \mathbf{M} (\ddot{\mathbf{q}} - \ddot{\mathbf{q}}_d)\}. \quad (5)$$

Using (5), we will derive an explicit relation $\mathbf{u} = \mathbf{u}(\mathbf{Q}_d)$. In this light, let us substitute (4) (where $\ddot{\mathbf{q}}$ is calculated using $\mathbf{Q}_u = \mathbf{E}\mathbf{u}$ while $\ddot{\mathbf{q}}_d$ is calculated using $\mathbf{Q}_u = \mathbf{Q}_d$) into (5) to obtain an explicit quadratic program for $\mathbf{u}$ as

$$\mathbf{u} = min\{\mathbf{u} \in \Re^m : \frac{1}{2}\mathbf{u}^T \mathbf{A}_u^T \mathbf{A}_u \mathbf{u} - \mathbf{b}_u^T \mathbf{A}_u \mathbf{u}\}, \quad (6)$$

where $\mathbf{A}_u = \mathbf{N}(\mathbf{R}^{-1})^T\mathbf{E}$ and $\mathbf{b}_u = \mathbf{N}(\mathbf{R}^{-1})^T\mathbf{Q}_d$ while $\mathbf{N} = \mathbf{I} - \mathbf{C}^+\mathbf{C} \in \Re^{n\times n}$ is a symmetric projection operator to the null space of the weighted constraint matrix $\mathbf{C}$. Considering the fact that $\mathbf{N}$ is in general rank deficient, a particular solution to (6) can be defined as:

$$\mathbf{u} = (\mathbf{N}(\mathbf{R}^{-1})^T\mathbf{E})^+ \mathbf{N}(\mathbf{R}^{-1})^T\mathbf{Q}_d. \quad (7)$$

The solution expressed by (7) can be used to compute joint torques regardless of whether the robot is underactuated or overactuated through a considered motion phase. Specifically, if the number of control inputs is equal or greater than the number of degrees of freedom of the robot, the solution to (7) satisfies the matching dynamics criterion (i.e., $\ddot{\mathbf{q}} = \ddot{\mathbf{q}}_d$), while also minimizing the squared Euclidean norm of $\mathbf{u}$. On the other hand, if the biped is underactuated, (7) minimizes the acceleration energy between the desired and the actual motion via the Gauss principle. In the present context, we expect any uncontrollable motion, if present, to occur only for brief periods (i.e., for periods much shorter than the characteristic times associated with the biped dynamics). As was recognized through numerous simulation this condition ensures stable realization of the underactuated motion phases.

IV. Implementation on a Seven-Link Biped

We illustrate and further describe the proposed approach via implementation and simulation on the seven-link biped presented in Fig.1.

A. Choice of Control

As previously described, we impose seven state-dependent torques on the biped, each of which can be constructed from energetically passive elements with fixed equilibrium points. These include an angular torque on the torso, state-dependent alternating angular torques on the thighs (both with respect to the inertial reference frame), and state-dependent torques on knees and ankles, defined with respect to the respective adjacent links. The simplest construction for these torques is the combination of a linear spring (with a fixed equilibrium point) and linear damper. Using these elements, the vector of desired generalized control forces can be expressed as:

$$\mathbf{Q}_d = -\mathbf{K}_d(\boldsymbol{\phi} - \boldsymbol{\phi}_d) - \mathbf{B}_d\dot{\boldsymbol{\phi}}, \quad (8)$$

where $\mathbf{K}_d$ is the stiffness matrix, $\mathbf{B}_d$ is the damping matrix, $\boldsymbol{\phi} = [q_3, q_4, q_5 - q_4, q_6 - q_5 + \pi/2, q_7, q_8 - q_7, q_9 - q_8 + \pi/2]^T$, and $\boldsymbol{\phi}_d = [\theta_b, \theta_l^r, 0, \theta_a^r, \theta_l^l, 0, \theta_a^l]^T$ defines the equilibrium point of each spring. The parameters that define $\mathbf{Q}_d$ for the seven-link biped are shown schematically in Fig.2 (where the right and left side parameters are indicated with superscripts).

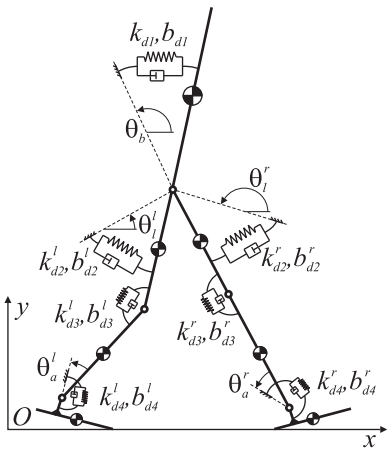

Fig. 2. Schematic representation of the control elements.

B. Event Driven State Logic

As previously mentioned, leg oscillation is generated by application of alternating torques applied to each thigh segment. This alternation is switched based on an event

driven finite state structure. Specifically, heel strike induces application of the hip torque that attracts the thigh toward a hip extension configuration, while the heel off event (i.e., when the heel leaves the ground) switches the hip torque to one that attracts the thigh towards a hip flexion configuration. In addition to these two states, two additional states are used to facilitate stable locomotion. Specifically, following the toe-off event (when the swing foot is entirely in the air), the swing leg ankle equilibrium point (i.e., angle of attraction) is moved to a slightly flexed position, which enhances ground clearance during swing. The final state, defined by the knee reaching full extension, is used to retain the knee at full extension. Thus, the gait controller consists of four states, as illustrated in Fig.3. Note that the states apply independently to each leg, and do not apply at all to the torque acting on the torso. As such, (for each leg), state one consists of stance, state two is initiated by heel-off, state three initiated by toe-off, state four initiated by full knee extension, and the leg is returned to state one by heel strike.

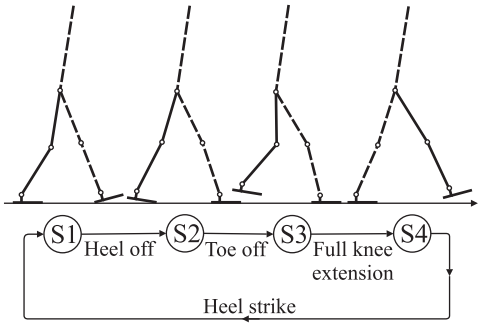

Fig. 3. State flow diagram. The presented state-event chart corresponds to the solid leg.

C. Simulation

For the biped illustrated in Fig.1, the associated geometric and inertial parameters normalized to a body height L and mass M, as given by [23], are listed in Table I. For purposes of control implementation and simulation, the biped was parameterized according to the values listed in Table I using a height $L = 1.8\ m$ and a mass $M = 75\ kg$. The simulation was conducted by utilizing the desired generalized force vector described in (8), and by using the joint torque control solution (7). For the (adult) human-scale anthropomorphic biped, the control parameters used for an approximately normal walking speed are listed in Table II (where the upper index $(*) = r/l$ represents the right or left leg, respectively). A stroboscopic image of the motion results of this controller, simulated over a period of $t \in [0, 10]s$, is shown in Fig.4. The corresponding real-time video of the resulting gait is included in the supporting material. For the simulation shown, the initial configuration of the biped was (starting at rest) in the double-support phase with both feet flat on the ground. The average forward walking speed for this simulation was $0.88m/s$.

Multiple possibilities exist for varying the control parameter set to achieve stable locomotion with different walking

TABLE I

GEOMETRIC AND INERTIAL PARAMETERS, WINTER [23].

Description	no. $(*)$	l_*/L	l_{c*}/l_*	m_*/M	r_*/l_*
Upper body	1	0.288	0.626	0.6780	0.496
Thigh	2	0.245	0.433	0.1000	0.323
Shank	3	0.246	0.433	0.0465	0.302
Foot	4	0.152	0.250	0.0145	0.475
Foot geometry			a/l_4	b/l_4	h/L
			0.75	0.25	0.039

TABLE II

CONTROLLER PARAMETERS; $k^*_{d()}[Nm]$, $b^*_{d()}[Nms]$, $\theta^*_{()}[deg]$.

States	k_{d1}	k^*_{d2}	k^*_{d3}	k^*_{d4}	b_{d1}	b^*_{d2}	b^*_{d3}	b^*_{d4}
1	400	750	30	20	50	300	5	15
2	400	70	30	20	50	1	5	15
3	400	70	0	5	50	1	1	1
4	400	0	30	5	50	0	5	1

States	1	2	3	4
θ_b	85			
θ^*_l	68	122	122	–
θ^*_a	0	0	10	0

speeds. A couple intuitive parameters that can be varied to influence the walking speed are the hip stiffness during stance (i.e., k_{d2} in state one), and the desired upper body angle θ_b. Figures 5 and 6 show stroboscopic images of the biped walking at faster and slower walking speeds (relative to Fig.4), respectively, both simulated over a period of $t \in [0, 10]s$, and both of which were generated by utilizing the same control parameter set given in Table II, but with different values for the hip stiffness at stance k_{d2} and the upper body angle θ_b. Specifically, to achieve these gaits, the parameters were set to $k_{d2} = 800Nm$, $\theta_b = 82.5^o$ and $k_{d2} = 655Nm$, $\theta_b = 87.5^o$ for the faster and slower gait respectively. The faster gait, which is shown in Fig.5 starting from rest at an initial condition of double-support (with the forward heel on the ground and the backward toe on the ground), is characterized by an average walking speed of $0.96m/s$. The slower gait, which is shown in Fig.6 starting from rest at an initial condition of single-support with the foot flat on the ground, is characterized by an average walking speed of $0.6m/s$. Corresponding real-time videos of these simulations are included in the supporting material.

Figure 7 shows the respective forward velocities (of the center of mass of the torso) at each of the three walking speeds. The corresponding time evolution of the upper body angle are depicted in Fig.8. As can be seen in the figure, the torso for each case starts at an upper body posture away from the sustained limit cycle, and in each case converges within a few steps to a stable steady-cycle.

As was outlined in the paper, the presented control approach is designed not to suppress to natural dynamics of the robot. A direct consequence is that the simulated motions have natural human style. Beyond this qualitative characteristic, the efficiency of dynamic walking should be improved

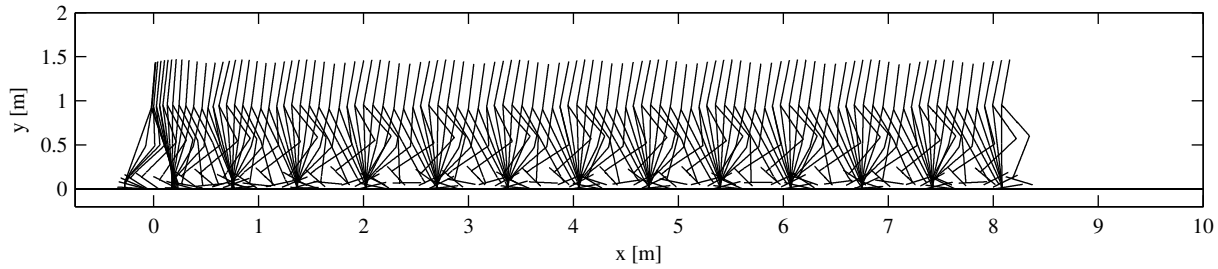

Fig. 4. Stroboscopic view of dynamic walking with $0.88m/s$ average forward speed. The motion is started from double support with both feet flat on the ground, $\mathbf{q}(0) = [0, 1.24, 1.5, 1.86, 1.86, 0, 1.23, 1.23, 0]^T$, $\dot{\mathbf{q}}(0) = \mathbf{0}$.

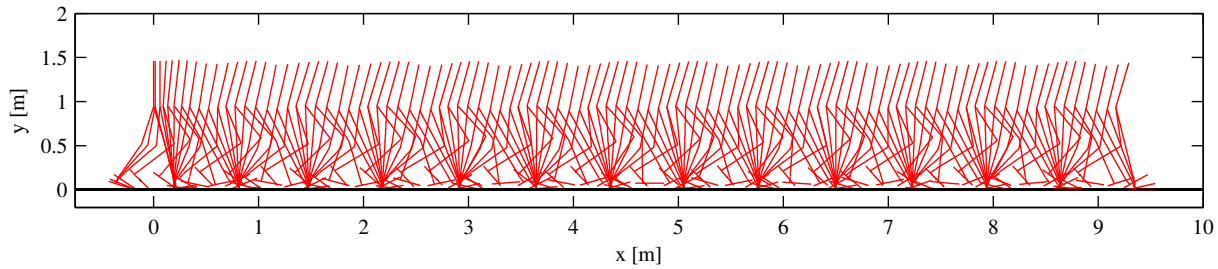

Fig. 5. Stroboscopic view of dynamic walking with $0.96m/s$ average forward speed. The motion is started from double support phase while only the forward heel and the backward toe are on the ground, $\mathbf{q}(0) = [0, 1.27, 1.57, 1.82, 1.78, 0.2, 1.31, 1.04, -0.35]^T$, $\dot{\mathbf{q}}(0) = \mathbf{0}$.

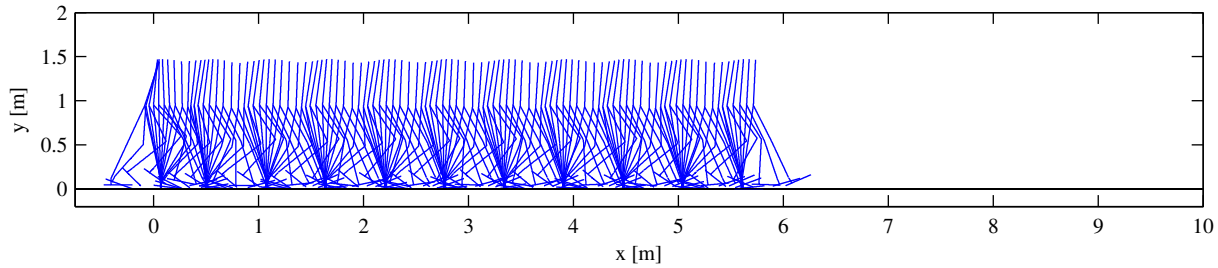

Fig. 6. Stroboscopic view of dynamic walking with $0.6m/s$ average forward speed. The motion is started from single support with the forward foot flat on the ground, $\mathbf{q}(0) = [0, 1.25, 1.3, 1.75, 1.75, 0, 1.2, 1.2, 0]^T$, $\dot{\mathbf{q}}(0) = \mathbf{0}$.

relative to a ZMP-based approach. The efficiency of gait can be characterized by the specific mechanical cost of transport, c_{mt}=(mech. energy)/(weight $\times$ distance traveled) [24]. Based on the simulation shown in Fig.4, the calculated mechanical cost of transport of the proposed approach is $c_{mt} = 0.2$. Comparatively, the specific mechanical cost of transport of the ZMP-based Honda Asimo is estimated as $c_{mt} = 1.6$ [11], while the cost of transport of the actuator-assisted Cornell dynamic walker is $c_{mt} = 0.05$ [11]. While these numbers may not be particularly accurate estimates, they support our claim by which utilization of the proposed control approach can provide energetic advantage over usual ZMP-based trajectory tracking approaches. The order of magnitude difference in the estimated values also provide an intuitive prediction by which using closed-loop control on all joints may unlikely to be energetically competitive with actuator-assisted passive dynamic walkers, although walking under closed-loop control is expected to be considerably more robust and versatile.

D. Comments on the Proposed Approach

Based on our experience with simulation of the biped was not particularly sensitive to initial conditions. Stable walking is achievable with different foot contact configuration, see Figs.4-6, by having the upper body in different initial angular position, see Fig.8, with a relatively large range of control parameters. Differing sets of control parameters result in a differing character of gait, some of which appear more natural and efficient than others. Other sets of parameters generate gaits that appear either more relaxed or more deliberate. There also obviously exists a large space of parameters that fail. These failures are mainly due to lack of coordination, which result in a stumble and ensuing fall. Beyond the presented results the authors conducted numerous simulations to evaluate the robustness and versatility of the presented walking controller. The results showed that the current walking simulations can handle in average 10% variation with respect to model parameters, specifically $\mathbf{M}$ and $\mathbf{A}$; downhill and uphill walk was achieved on $\pm 5^o$ slope; robustness with respect to forward and backward push

type disturbance was verified with $200N$ force applied at the center of mass of the upper body for $0.2s$ duration. Numerical results also indicate that by changing k_{d2} and θ_b one can obtain safe and smooth transitions between different walking gaits.

For the simulations presented here, the control parameters which have clear physical meaning, see Fig.2, were selected by hand tuning and intuition.

V. CONCLUSION

The authors have proposed an approach for locomotion control that allows biped walking in natural human style. Rather than prescribe kinematic trajectories, the approach is based on the prescription of state dependent torques that "encourage" patterned movement through the natural dynamics of the biped. The control method is implemented in simulation on an anthropomorphic biped, which is shown to quickly converge to a natural-looking gait limit cycle with various control parameters and different initial conditions. The authors also show that walking speed can be altered by varying two intuitive controller parameters. The mechanical cost of transport calculated on a representative dynamic walk verifies that the presented approach allows control which works with instead of against the robot dynamics. Experimental validation of the presented approach on a 7-link biped robot built at the Vanderbilt University Center of Inteligent Mechatronics: http://research.vuse.vanderbilt.edu/cim, is part of our future work.

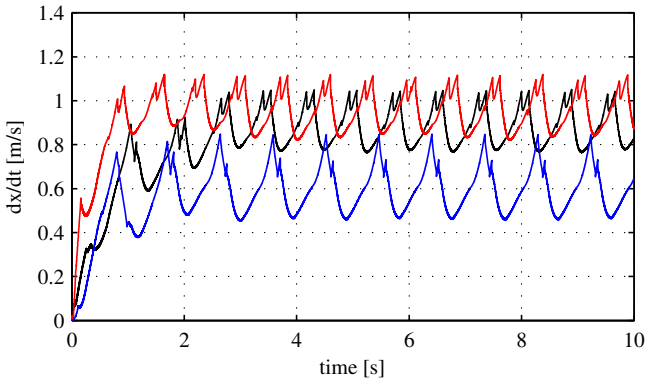

Fig. 7. Forward velocity of the upper body CoM for walking at three different speeds.

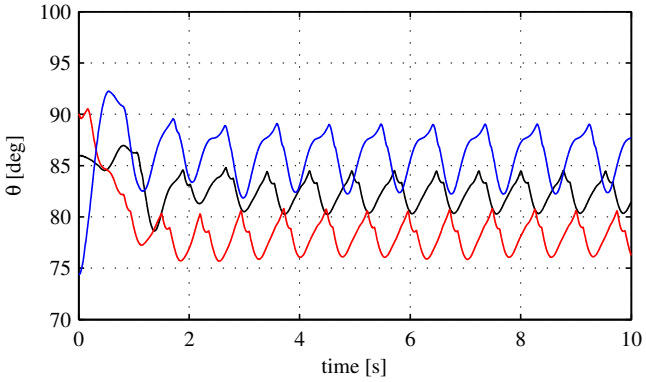

Fig. 8. Upper body angle during walking at three different speeds. The vertical upright position corresponds to 90^o.

REFERENCES

[1] M. Vukobratović and J. Stepanenko, "On the stability of antropometric systems," *Mathematical Bioscience*, vol. 15, no. 1, pp. 1–37, 1972.

[2] M. Vukobratović, B. Borovac, D. Šurla, and D. Stokić, *Biped Locomotion*. Springer Verlag, 1990.

[3] K. Hirai, M. Hirose, Y. Haikawa, and T. Takenaka, "The development of. honda humanoid robot," *Proceedings of the 1998 IEEE ICRA*, pp. 1321–1326, 1998.

[4] Q. Huang, K. Yokoi, S. Kajita, K. Kaneko, H. Arai, N. Koyachi, and K. Tanie, "Planning walking patterns for a biped robot," *IEEE Transactions on Robotics and Automation*, vol. 17, no. 3, pp. 208–289, 2001.

[5] S. Kagami, T. Kitagawa, K. Nishiwaki, T. Sugihara, M. Inaba, and H. Inoue, "A fast dynamically equilibrated walking trajectory generation method of humanoid robot," *Autonomuous Robots*, vol. 12, pp. 71–82, 2002.

[6] C. Chevallereau, D. Djoudi, and J. W. Grizzle, "Stable bipedal walking with foot rotation through direct regulation of the zero moment point," *IEEE Transactions on Robotics*, vol. 24, no. 2, pp. 390–401, 2008.

[7] A. D. Kuo, "Choosing your steps carefully," *IEEE Robotics and Automation Magazine*, vol. 14, no. 2, pp. 18–29, 2007.

[8] T. McGeer, "Passive dynamic walking," *The International Journal of Robotics Research*, vol. 9, no. 2, pp. 62–82, 1990.

[9] M. J. Coleman and A. Ruina, "An uncontrolled walking toy that cannot stand still," *Physical Review Letters*, vol. 80, no. 16, pp. 3658–3661, 1998.

[10] M. Garcia, A. Ruina, A. Chatterjee, and M. Coleman, "The simplest walking model: Stability, complexity, and scaling," *Journal of Biomechanical Engineering*, vol. 120, no. 2, pp. 281–288, 1998.

[11] S. Collins, A. Ruina, R. Tedrake, and M. Wisse, "Efficient bipedal robots based on passive dynamic walkers," *Science Magazine*, vol. 307, pp. 1082–1085, 2005.

[12] M. Wisse, G. Feliksdal, J. van Frankenhuyzen, and B. Moyer, "Passive-based walking robot: Denis a simple efficient and lightweight biped," *IEEE Robotics and Automation Magazine*, vol. 14, no. 2, pp. 52–62, 2007.

[13] J. W. Grizzle, G. Abba, and F. Plestan, "Asymptotically stable walking for biped robots: Analysis via systems with impulse effects," *IEEE Transactions on Automatic Control*, vol. 46, no. 1, pp. 51–64, 2001.

[14] F. Plestan, J. W. Grizzle, E. R. Westervelt, and G. Abba, "Stable walking of a 7-dof biped robot," *IEEE Transactions on Robotics and Automation*, vol. 19, no. 4, pp. 653–668, 2003.

[15] E. R. Westervelt, J. W. Grizzle, and D. E. Koditschek, "Hybrid zero dynamics of planar biped walkers," *IEEE Transactions on Automatic Control*, vol. 48, no. 1, pp. 42–56, 2003.

[16] C. C. de Wit, "On the concept of virtual constraints as a tool for walking robot control and balancing," *Annual Reviews in Control*, vol. 28, pp. 157–166, 2004.

[17] J. Pratt, C. M. Chew, A. Torres, P. Dilworth, and G. Pratt, "Virtual model control: An intuitive approach for bipedal locomotion," *The International Journal of Robotics Research*, vol. 20, pp. 129–143, 2001.

[18] F. E. Udwadia and R. E. Kalaba, "A new perspective on constrained motion," *Proceedings of the Royal Society of London* A, vol. 439, pp. 407–410, 1992.

[19] F. E. Udwadia and R. E. Kalaba, *Analytical Dynamics: A New Approach*. Cambridge University Press, Cambridge, England, 1996.

[20] C. F. Gauss, "Über ein neues algemeines grundgesetz der mechanik," *Zeitschrift für die reine und angewandte Mathematik*, vol. 4, pp. 232–235, 1829.

[21] G. Golub and C. V. Loan, *Matrix Computations*. The John Hopkins University Press, 3 ed., 1996.

[22] A. Ben-Israel and T. N. E. Greville, *Generalized Inverse: Theory and Applications*. Springer, 2003.

[23] D. A. Winter, *Biomechanics and Motor Control of Human Movement*. Wiley-Interscience, New York, 2 ed., 1990.

[24] G. Gabrielli and T. von Kármán, "What price speed?: Specific power required for propulsion of vehicles," *Mechanical Engineering*, vol. 72, no. 10, pp. 775–781, 1950.